

Quantum Nonlocality for a Mixed Entangled Coherent State

D. Wilson, H. Jeong and M. S. Kim

School of Mathematics and Physics, Queen's University, Belfast BT7 1NN, United Kingdom

(October 25, 2018)

Abstract

Quantum nonlocality is tested for an entangled coherent state, interacting with a dissipative environment. A pure entangled coherent state violates Bell's inequality regardless of its coherent amplitude. The higher the initial nonlocality, the more rapidly quantum nonlocality is lost. The entangled coherent state can also be investigated in the framework of 2×2 Hilbert space. The quantum nonlocality persists longer in 2×2 Hilbert space. When it decoheres it is found that the entangled coherent state fails the nonlocality test, which contrasts with the fact that the decohered entangled state is always entangled.

arXiv:quant-ph/0109121v2 28 Jan 2002

I. INTRODUCTION

Einstein, Podolsky, and Rosen proposed a thought experiment to test the local realism properties of quantum mechanics [1]. An inequality imposed by a local hidden variable theory was suggested by Bell [2], which enables a quantitative test concerning the controversy of local realism versus quantum mechanics in a real laboratory. Various versions of Bell's inequality [3,4] followed the original one, and experiments have been performed testing local realism [5]. In spite of successful experimental results, it has been pointed out that there remain two possible loopholes. One is called the lightcone loophole that might allow local realistic interpretation. Some experiments have been performed with strict relativistic separation between measurements to close this loophole [6]. The other is the detection loophole due to detection inefficiency. According to this loophole, there is a possibility that the detected subensemble violates Bell's inequality even though the whole ensemble satisfies it. Some authors generalised Bell's inequality to the case of inefficient detection [4,7,8] and other proposals have been made [9] to close the detection loophole. An experiment on nonlocality has been performed with an efficient detection [10].

The nonlocality test can be performed on an entangled system composed of two coherent systems [11]. This entangled system can be used as a quantum entangled channel for quantum information transfer. The entangled coherent state can be generated using a coherent light propagating through a nonlinear medium [12] and a 50-50 beam splitter as shown in Fig. 1. There have also been proposals to entangle fields in two spatially separated cavities [13]. The entangled coherent state and its usage for quantum information processing [14–17], teleportation [14,16,17] and entanglement concentration [17] have all been studied recently.

In this paper, we study nonlocality of an entangled coherent state using photon parity measurement. We first investigate the nonlocality of a pure entangled coherent state, and move on to the dynamic behavior of nonlocality for a decohered entangled coherent state in a vacuum environment. The dynamic behaviour is also investigated in the framework of 2×2 Hilbert space and the results are compared. It is found that nonlocality of a decohered

entangled coherent state persists longer when it is considered in 2×2 space.

II. NONLOCALITY FOR AN ENTANGLED COHERENT STATE

We are interested in nonlocality of an entangled coherent state

$$|C\rangle_{12} = \frac{1}{\sqrt{N}}(|\alpha\rangle_1 |-\alpha\rangle_2 + e^{i\varphi} |-\alpha\rangle_1 |\alpha\rangle_2), \quad (1)$$

where $\alpha = \alpha_r + i\alpha_i$ is a complex amplitude, φ is a real local phase factor, and N is a normalisation factor. By applying local unitary transformations any state in the form of

$$|\Psi\rangle_{12} = \frac{1}{\sqrt{N}}(|\beta\rangle_1 |\gamma\rangle_2 + e^{i\varphi} |\gamma\rangle_1 |\beta\rangle_2) \quad (2)$$

with arbitrary amplitudes β and γ can be transformed to a form like that of Eq. (1) up to a global phase factor. Applying displacement operators $D_1(x)D_2(x)$, where $x = x_r + ix_i$ is complex, the entangled coherent state (2) becomes

$$D_1(x)D_2(x)|\Psi\rangle_{12} = \frac{e^{i\phi}}{\sqrt{N}}(|\alpha\rangle_1 |-\alpha\rangle_2 + e^{i\varphi} |-\alpha\rangle_1 |\alpha\rangle_2) \quad (3)$$

with $x = -\frac{1}{2}(\beta + \gamma)$, $\alpha = \beta + x = -(\gamma + x)$, and $\phi = x_i\beta_r - x_r\beta_i + x_i\alpha_r - x_r\alpha_i$. Here the displacement operator is defined as $D(x) = \exp(xa^\dagger + x^*a)$, where a and a^\dagger are annihilation and creation operators [18]. In this paper, we consider the nonlocality of entangled coherent states

$$|C_\pm\rangle = \frac{1}{\sqrt{N_\pm}}(|\alpha\rangle |-\alpha\rangle \pm |-\alpha\rangle |\alpha\rangle) \quad (4)$$

where N_\pm are normalisation factors and α is assumed to be real for simplicity.

The type of quantum observable to be measured is a crucial factor in the nonlocality test. Banaszek and Wódkiewicz developed a Wigner function representation of the Bell-Clauser, Horne, Shimony and Holt (CHSH) [3] inequality using a two-mode parity operator $\Pi(\alpha, \beta)$ as a quantum observable [19,20]. The two-mode parity operator $\Pi(\alpha, \beta)$ is defined as

$$\Pi(\alpha, \beta) = D_1(\alpha)D_2(\beta)\Pi D_1^\dagger(\alpha)D_2^\dagger(\beta), \quad (5)$$

where

$$\Pi = \Pi_{e1} \otimes \Pi_{e2} - \Pi_{e1} \otimes \Pi_{o2} - \Pi_{o1} \otimes \Pi_{e2} + \Pi_{o1} \otimes \Pi_{o2}, \quad (6)$$

with

$$\Pi_e = \sum_n^{\infty} |2n\rangle\langle 2n|, \quad \Pi_o = \sum_n^{\infty} |2n+1\rangle\langle 2n+1|. \quad (7)$$

The Bell-CHSH inequality is then

$$|\mathcal{B}| = |\langle \Pi(\alpha, \beta) + \Pi(\alpha, \beta') + \Pi(\alpha', \beta) - \Pi(\alpha', \beta') \rangle| \leq 2, \quad (8)$$

where we call $|\mathcal{B}|$ the Bell measure. The displacement operation can be effectively performed using a beam splitter with the transmission coefficient close to one and a strong coherent state being injected into the other input port [20]. The two-mode Wigner function at a given phase point described by α and β is

$$W(\alpha, \beta) = \frac{4}{\pi^2} \text{Tr}[\rho \Pi(\alpha, \beta)], \quad (9)$$

where ρ is the density operator of the field. From Eqs.(8) and (9), we obtain the Wigner representation of Bell's inequality

$$|\mathcal{B}| = \frac{\pi^2}{4} |W(\alpha, \beta) + W(\alpha, \beta') + W(\alpha', \beta) - W(\alpha', \beta')| \leq 2. \quad (10)$$

The Wigner function of an entangled coherent state is obtained from the Fourier transform of its characteristic function

$$C(\eta, \xi) = \text{Tr}[\rho D_1(\eta) D_2(\xi)]. \quad (11)$$

Banaszek and Wódkiewicz used their Wigner function based Bell measure with $\alpha = \beta = 0$. We consider all four variables α, β, α' and β' in our investigation of the Wigner function based Bell measure as shown in Eq. (10) to test nonlocality more generally. The maximum Bell-CHSH violation using Banaszek and Wódkiewicz's version is approximately 2.19 for two-mode squeezed states [19,22] and 2.5 for entangled coherent states as shown in Fig. 2.

However, for the generalised Bell measure in Eq. (10), both two-mode squeezed states [23] and entangled coherent states have a maximal Bell-CHSH violation of $2\sqrt{2}$ (as shown in Fig. 2).

The entangled coherent states $|C_-\rangle$ and $|C_+\rangle$ violate the Bell inequality regardless of the size of the amplitude, $\alpha > 0$. As the amplitude α increases the Bell measure tends towards a maximum of $2\sqrt{2}$.

It is interesting to note that the Bell measure for the $|C_-\rangle$ state takes a higher value than for the $|C_+\rangle$ state. If the number state representation of the coherent state is [18]

$$|\alpha\rangle = \sum_n \frac{e^{-|\alpha|^2/2} \alpha^n}{\sqrt{n!}} |n\rangle \quad (12)$$

which means that, in the limit of small coherent amplitude α ,

$$|\pm\alpha\rangle \approx e^{-|\alpha|^2/2} [|0\rangle \pm \alpha|1\rangle]. \quad (13)$$

Substituting this into the entangled coherent states $|C_+\rangle$ and $|C_-\rangle$ we find

$$\begin{aligned} |C_+\rangle &\propto |0\rangle|0\rangle - \alpha^2|1\rangle|1\rangle \\ |C_-\rangle &\propto \alpha(|1\rangle|0\rangle - |0\rangle|1\rangle) \end{aligned} \quad (14)$$

When α is small $|C_+\rangle \rightarrow |0\rangle|0\rangle$. As the weights of $|0\rangle|0\rangle$ and $|1\rangle|1\rangle$ are radically different $|C_+\rangle$ is only minimally entangled. However the two component states $|0\rangle|1\rangle$ and $|1\rangle|0\rangle$ are equally weighted for $|C_-\rangle$ which gives optimal entanglement. A pure entangled state always violates nonlocality [24]. Any entangled coherent state in a form as given in Eq. (4) is found to be nonlocal. We conjecture that any entangled coherent state as given in Eq. (2) also has nonlocality except when $\beta = \gamma$, *i.e.*, when the state is a product state.

The results shown in Fig. 2 were obtained from a numerical consideration of the Bell measure (10). In analogy with the work carried out in [22] we imposed the condition $\mathcal{B}(|\alpha\rangle, |\beta\rangle, |\alpha'\rangle, |\beta'\rangle) = \mathcal{B}(|\beta\rangle, |\alpha\rangle, |\beta'\rangle, |\alpha'\rangle)$. The method of steepest descent [25] was used to find the maximum of the Bell measure under our assumptions.

III. DYNAMICS OF NONLOCALITY

A quantum system loses its quantum characteristics if it is open to the world. We modelled an entangled coherent state interacting with a dissipative environment (two independent vacuum reservoirs). To study the dynamics of nonlocality of continuous variable entangled coherent states it is necessary to find an expression of the time-dependent Bell-CHSH measure. This in turn means finding an expression for the time-dependent decohered Wigner function.

The quantum channel decoheres when it interacts with its environment and becomes a mixed state of its density operator $\rho(\tau)$, where τ is the decoherence time. To know the time dependence of $\rho(\tau)$, we have to solve the master equation

$$\frac{\partial \rho}{\partial \tau} = \hat{J}\rho + \hat{L}\rho ; \quad \hat{J}\rho = \gamma \sum_i a_i \rho a_i^\dagger, \quad \hat{L}\rho = -\frac{\gamma}{2} \sum_i (a_i^\dagger a_i \rho + \rho a_i^\dagger a_i) \quad (15)$$

where a_i and a_i^\dagger are the annihilation and creation operators for the field mode i and γ is the decay constant. We have assumed that each field mode is coupled to its environment at the same coupling rate γ . The formal solution of the master equation (15) can be written as

$$\rho(t) = \exp[(\hat{J} + \hat{L})\tau]\rho(0). \quad (16)$$

which leads to the solution for the initial single-mode dyadic $|\alpha\rangle\langle\beta|$

$$\exp[(\hat{J} + \hat{L})\tau]|\alpha\rangle\langle\beta| = \langle\beta|\alpha\rangle^{1-t^2}|\alpha t\rangle\langle\beta t| \quad (17)$$

where $t = e^{-\frac{1}{2}\gamma\tau}$. In this paper, we introduce a dimensionless normalised interaction time r which is related to t by the expression $r = \sqrt{1-t^2}$. When $\tau = 0, t = 1$ and $r = 0$. As $\tau \rightarrow \infty, t \rightarrow 0$ and $r \rightarrow 1$.

After solving the master equation (15) for the initial entangled coherent state, the time-dependent density operator $\rho(\tau)$ is obtained. Substituting $\rho(\tau)$ into Eq.(11), we calculate the characteristic function and its Fourier transform to obtain the Wigner function for the decohered entangled coherent state. Once again the results shown in Figs. 3-4 were

obtained using the method of steepest descent to find the maximum value of the Bell measure under our assumptions. The same symmetrical consideration as before (namely $\mathcal{B}(|\alpha\rangle, |\beta\rangle, |\alpha'\rangle, |\beta'\rangle) = \mathcal{B}(|\beta\rangle, |\alpha\rangle, |\beta'\rangle, |\alpha'\rangle)$) was imposed.

From Figs. 3-4 it is obvious that as the entangled coherent state interacts with its environment it fails the nonlocality test. From Fig. 3 it can be seen that as the coherent amplitude α increases the initial nonlocality increases and the rate of loss of nonlocality increases. The larger the initial amplitude, *i.e.*, the larger the initial nonlocality, the more rapid the loss of nonlocality occurs, *i.e.*, the shorter the duration of the nonlocality. As $r \rightarrow 1$, in Fig. 3, ρ becomes a product of two vacuum states and the Bell measure approaches the value 2.

We can see in Fig. 4 that the $|C_+\rangle$ state of the coherent amplitude $\alpha = 0.1$ has a long duration of nonlocality ($r \approx 0.375$). The duration of the nonlocality can be increased by decreasing the coherent amplitude.

IV. NONLOCALITY TEST IN 2×2 DIMENSIONAL HILBERT SPACE

Entangled coherent states can be considered in 2×2 dimensional Hilbert space [17], where $|C_-\rangle$ shows maximal entanglement regardless of the value of α [15]. In this section, we will investigate nonlocality and the dynamics of the entangled coherent state $|C_-\rangle$ in a vacuum environment within the framework of 2×2 Hilbert space (see also the discussions in ref. [26]).

We consider two orthogonal states

$$|e\rangle = \frac{1}{\sqrt{\mathcal{N}_+}}(|\alpha\rangle + |-\alpha\rangle), \quad (18)$$

$$|d\rangle = \frac{1}{\sqrt{\mathcal{N}_-}}(|\alpha\rangle - |-\alpha\rangle) \quad (19)$$

where $\mathcal{N}_+ = 2 + 2e^{-2\alpha^2}$ and $\mathcal{N}_- = 2 - 2e^{-2\alpha^2}$ are normalisation factors. A two-dimensional Hilbert space can be spanned using these states as orthonormal bases. The entangled coherent state $|C_-\rangle$ can be represented in 2×2 dimensional Hilbert space as

$$|C_-\rangle_{12} = \frac{1}{\sqrt{2}}(|e\rangle_1|d\rangle_2 - |d\rangle_1|e\rangle_2), \quad (20)$$

where we recognise that $|C_-\rangle$ is maximally entangled.

The Bell-CHSH inequality for a bipartite spin- $\frac{1}{2}$ state $|\psi\rangle$ is $|\mathcal{B}| \leq 2$, where

$$\mathcal{B} = \langle \psi | \vec{a} \cdot \vec{\sigma}_1 \otimes \vec{b} \cdot \vec{\sigma}_2 + \vec{a} \cdot \vec{\sigma}_1 \otimes \vec{b}' \cdot \vec{\sigma}_2 + \vec{a}' \cdot \vec{\sigma}_1 \otimes \vec{b} \cdot \vec{\sigma}_2 - \vec{a}' \cdot \vec{\sigma}_1 \otimes \vec{b}' \cdot \vec{\sigma}_2 | \psi \rangle \quad (21)$$

and \vec{a} , \vec{a}' , \vec{b} and \vec{b}' are three-dimensional unit vectors and σ 's are Pauli matrices [27]. The unit vectors determine the directions of σ -operators which are measurement observables. They are usually realised by rotating the measurement apparatuses at both sides. The effect of these unit vectors can also be realised by local unitary operations on both particles of the pair independently, fixing the direction of the measurement apparatuses so that the measurement operator becomes $\sigma_{z1} \otimes \sigma_{z2}$.

We first consider ideal conditions for the nonlocality test. Assume $|e\rangle$ and $|d\rangle$ can be perfectly discriminated with eigenvalues 1 and -1 by an ideal measurement operator $O_s = |e\rangle\langle e| - |d\rangle\langle d|$, where the operator O_s is an analogy to σ_z in a spin- $\frac{1}{2}$ system. If an ideal rotation such as $R_x(\theta)$ around an axis,

$$\begin{aligned} R_x(\theta)|e\rangle &= \cos \theta |e\rangle + i \sin \theta |d\rangle, \\ R_x(\theta)|d\rangle &= i \sin \theta |e\rangle + \cos \theta |d\rangle, \end{aligned} \quad (22)$$

can be performed on the particles of both sides by two local measurements O_{s1} and O_{s2} . Under these conditions, it can be proved that the entangled coherent state $|C_-\rangle$ maximally violates the Bell-CHSH inequality regardless of the value of α , *i.e.*, $|\mathcal{B}|_{max} = 2\sqrt{2}$.

The dynamic change of nonlocality for the entangled coherent state can be obtained from its time-dependent density matrix. Assuming vacuum environment, it is possible to restrict our discussion in 2×2 dimensional Hilbert space even for the mixed case. The basis vectors in Eqs. (18) and (19) now should be

$$|e(\tau)\rangle = \frac{1}{\sqrt{\mathcal{N}_+(\tau)}}(|t\alpha\rangle + |-t\alpha\rangle), \quad (23)$$

$$|d(\tau)\rangle = \frac{1}{\sqrt{\mathcal{N}_-(\tau)}}(|t\alpha\rangle - |-t\alpha\rangle), \quad (24)$$

where $\mathcal{N}_+(\tau) = 2 + 2e^{-2t^2\alpha^2}$ and $\mathcal{N}_-(\tau) = 2 - 2e^{-2t^2\alpha^2}$. Although $|e(\tau)\rangle$ and $|d(\tau)\rangle$ are time-dependent, they always remain orthogonal until, $\tau \rightarrow \infty$.

With use of the master equation (15) we find the mixed density matrix $\rho_-(\tau)$ as follows

$$\rho_-(\tau) = \frac{1}{4\mathcal{N}_+\mathcal{N}_-} \begin{pmatrix} A & 0 & 0 & D \\ 0 & C & -C & 0 \\ 0 & -C & C & 0 \\ D & 0 & 0 & E \end{pmatrix}, \quad (25)$$

where A , C , D and E are defined as

$$A = (1 - \Gamma)\mathcal{N}_+^2(\tau), \quad (26)$$

$$C = (1 + \Gamma)\mathcal{N}_+(\tau)\mathcal{N}_-(\tau), \quad (27)$$

$$D = -(1 - \Gamma)\mathcal{N}_+(\tau)\mathcal{N}_-(\tau), \quad (28)$$

$$E = (1 - \Gamma)\mathcal{N}_-^2(\tau), \quad (29)$$

$$\Gamma = \exp\{-4(1 - t^2)\alpha^2\}. \quad (30)$$

The maximal Bell-CHSH violation for a 2×2 dimensional state ρ is given in [28]

$$|\mathcal{B}|_{max} = 2\sqrt{M(\rho)}, \quad (31)$$

where $M(\rho)$ is the sum of the two larger eigenvalues of TT^\dagger and T is a 3×3 matrix whose elements are defined as $t_{nm} = \text{Tr}(\rho\sigma_m \otimes \sigma_n)$ with Pauli matrices represented by σ 's. Ideal measurement and rotation ability should be assumed again here to use this formula. The three eigenvalues of TT^\dagger for the mixed entangled coherent state ρ_- are

$$\frac{(C + D)^2}{4\mathcal{N}_+^2\mathcal{N}_-^2}, \quad \frac{(C - D)^2}{4\mathcal{N}_+^2\mathcal{N}_-^2}, \quad \frac{(A - 2C + E)^2}{16\mathcal{N}_+^2\mathcal{N}_-^2}, \quad (32)$$

from which $M(\rho_-)$ is obtained by calculating the sum of the two larger eigenvalues.

Fig. 5 shows $|\mathcal{B}|_{max}$ versus the dimensionless time $r(\tau)$. Initially, $\rho_-(\tau = 0)$ is maximally entangled regardless of α and $|\mathcal{B}|_{max}$ has the maximal value $2\sqrt{2}$. As interaction time increases, nonlocality decreases. For $\tau \rightarrow \infty$, ρ_- becomes a direct product of two coherent

states, which is a pure state, and $|\mathcal{B}|_{max}$ becomes 2. It is clear from Fig. 5 that the nonlocality persists longer in 2×2 Hilbert space than in continuous-variable space. We can see that the nonlocality of a given state varies according to the Hilbert space in which the state is considered, as entanglement also does [17].

It has already been found that the decohered state $\rho_-(\tau)$ always remains entangled in 2×2 Hilbert space [17]. This indicates that the mixed state $\rho_-(\tau)$ retains some amount of entanglement even after it loses its nonlocality. For pure states, it is true that any entangled state violates Bell's inequality [24]. On the other hand, it was shown that there are mixed states which are entangled but do not violate Bell's inequality [30]. Our model in 2×2 space is one example of that case.

Because the state $|e\rangle$ contains only even numbers of photons and $|d\rangle$ contains only odd numbers of photons, these two states are eigenstates of the operator $O_r = \Pi_e - \Pi_o$ which is known as the pseudo-spin operator [31], *i.e.*,

$$O_r|x_n\rangle = \lambda_n|x_n\rangle; \quad n = 1, 2 \quad (33)$$

$$\lambda_{1,2} = \pm 1; \quad |x_{1,2}\rangle = |e\rangle, |d\rangle, \quad (34)$$

by which $|e\rangle$ and $|d\rangle$ can be perfectly discriminated. The parameters $\lambda_{1,2}$ are eigenvalues of the pseudo-spin operator O_r and $|x_{1,2}\rangle$ are eigenvectors of the operator. The measurement for the nonlocality test is now $\Pi = O_{r1} \otimes O_{r2}$, which is in fact the same as the Π defined in Eqs. (6) and (7). Therefore, the nonlocality test in 2×2 space can be performed by the same parity measurement as in Eqs. (6) and (7). Note that there is no way to distinguish between O_r and O_s in our restricted Hilbert space.

If an ideal rotation R_x is possible for $|e\rangle$ and $|d\rangle$, the same structure as $\vec{a} \cdot \vec{\sigma}_1 \otimes \vec{b} \cdot \vec{\sigma}_2$ can be perfectly made by Π . Cochrane *et al.* [29] showed that rotation $R_x(\theta)$ can be approximately realised for $\alpha \gg 1$ by a displacement operator which can change the parity of the even state $|e\rangle$ and the odd state $|d\rangle$ [29]. When a displacement operator $D(i\epsilon)$, where ϵ is real, is applied to a given parity eigenstate it shows oscillations between $|e\rangle$ and $|d\rangle$.

To obtain the Bell function, we can calculate

$$P_e(\epsilon) = \langle e' | \Pi_e | e' \rangle = \frac{e^{\alpha^2 - \epsilon^2} \left\{ e^{2i\alpha\epsilon} \cosh[(\alpha + i\epsilon)^2] + e^{-2i\alpha\epsilon} \cosh[(\alpha - i\epsilon)^2] + 2 \cosh[\alpha^2 + \epsilon^2] \right\}}{2(1 + e^{2\alpha^2})}, \quad (35)$$

$$\tilde{P}_e(\epsilon) = \langle d' | \Pi_e | d' \rangle = \frac{e^{\alpha^2 - \epsilon^2} \left\{ e^{2i\alpha\epsilon} \cosh[(\alpha + i\epsilon)^2] + e^{-2i\alpha\epsilon} \cosh[(\alpha - i\epsilon)^2] - 2 \cosh[\alpha^2 + \epsilon^2] \right\}}{2(1 - e^{2\alpha^2})}, \quad (36)$$

$$I_e(\epsilon) = \langle e' | \Pi_e | d' \rangle = \frac{e^{\alpha^2 - \epsilon^2} \left\{ e^{2i\alpha\epsilon} \cosh[(\alpha + i\epsilon)^2] - e^{-2i\alpha\epsilon} \cosh[(\alpha - i\epsilon)^2] \right\}}{2\sqrt{1 - e^{-4\alpha^2}}}, \quad (37)$$

$$P_o(\epsilon) = \langle e' | \Pi_o | e' \rangle = 1 - P_e(\epsilon), \quad (38)$$

$$\tilde{P}_o(\epsilon) = \langle d' | \Pi_o | d' \rangle = 1 - \tilde{P}_e(\epsilon), \quad (39)$$

$$I_o(\epsilon) = \langle d' | \Pi_o | e' \rangle = -I_e(\epsilon), \quad (40)$$

where $|e'\rangle = D(i\epsilon)|e\rangle$ and $|d'\rangle = D(i\epsilon)|d\rangle$.

From the average values $P_e(\epsilon) = \langle e' | \Pi_e | e' \rangle$ and $\tilde{P}_e(\epsilon) = \langle d' | \Pi_e | d' \rangle$ shown in Fig. 6, which represent the probabilities for the measured state to have even parity, we can see oscillations due to $D(i\epsilon)$ in the even and odd states.

The Bell-CHSH inequality is then obtained using Eqs. (35) to (40),

$$\begin{aligned} \mathcal{B} = & \langle C_-(\epsilon_1, \epsilon_2) | \Pi | C_-(\epsilon_1, \epsilon_2) \rangle + \langle C_-(\epsilon_1, \epsilon'_2) | \Pi | C_-(\epsilon_1, \epsilon'_2) \rangle \\ & + \langle C_-(\epsilon'_1, \epsilon_2) | \Pi | C_-(\epsilon'_1, \epsilon_2) \rangle - \langle C_-(\epsilon'_1, \epsilon'_2) | \Pi | C_-(\epsilon'_1, \epsilon'_2) \rangle \end{aligned} \quad (41)$$

$$\begin{aligned} = & (2P_e(\epsilon_1) - 1)(\tilde{P}_e(\epsilon_2) + \tilde{P}_e(\epsilon'_2) - 1) + (2\tilde{P}_e(\epsilon_1) - 1)(P_e(\epsilon_2) + P_e(\epsilon'_2) - 1) \\ & + (2P_e(\epsilon'_1) - 1)(\tilde{P}_e(\epsilon_2) - \tilde{P}_e(\epsilon'_2)) + (2\tilde{P}_e(\epsilon'_1) - 1)(P_e(\epsilon_2) - P_e(\epsilon'_2)) \\ & + 4I_e(\epsilon_1)(I_e(\epsilon_2) + I_e(\epsilon'_2)) + 4I_e(\epsilon'_1)(I_e(\epsilon_2) - I_e(\epsilon'_2)), \end{aligned} \quad (42)$$

where $|C_-(\epsilon_1, \epsilon_2)\rangle = D_1(i\epsilon_1) \otimes D_2(i\epsilon_2) |C_-\rangle_{12}$. The nonlocality of this pure entangled coherent state is the same as the nonlocality of the four variable consideration shown in Fig. 2 (higher valued solid line).

For a mixed state, $\rho_-(\tau)$ is used to obtain the Bell function,

$$\mathcal{B} = \text{Tr}\{\rho_-(\tau; \epsilon_1, \epsilon_2)\Pi\} + \text{Tr}\{\rho_-(\tau; \epsilon_1, \epsilon'_2)\Pi\} + \text{Tr}\{\rho_-(\tau; \epsilon'_1, \epsilon_2)\Pi\} - \text{Tr}\{\rho_-(\tau; \epsilon'_1, \epsilon'_2)\Pi\}, \quad (43)$$

$$\rho_-(\tau; \epsilon_1, \epsilon_2) = D_1(i\epsilon_1) \otimes D_2(i\epsilon_2) \rho_-(\tau) D_1^\dagger(i\epsilon_1) \otimes D_2^\dagger(i\epsilon_2). \quad (44)$$

To calculate $\text{Tr}\{\rho_-(\tau; \epsilon_1, \epsilon_2)\Pi\}$, we need to use the redefined identity in the restricted Hilbert space,

$$\begin{aligned}
\mathbb{1}_r &= |e(\tau)\rangle_1|e(\tau)\rangle_{22}\langle e(\tau)|_1\langle e(\tau)| + |e(\tau)\rangle_1|d(\tau)\rangle_{22}\langle d(\tau)|_1\langle e(\tau)| \\
&\quad + |d(\tau)\rangle_1|e(\tau)\rangle_{22}\langle e(\tau)|_1\langle d(\tau)| + |d(\tau)\rangle_1|d(\tau)\rangle_{22}\langle d(\tau)|_1\langle d(\tau)| \\
&\equiv \sum_{n=1}^4 |X_n\rangle\langle X_n|, \tag{45}
\end{aligned}$$

which is not equal to the identity $\mathbb{1} = \frac{1}{\pi} \int d^2\alpha d^2\beta |\alpha\rangle|\beta\rangle\langle\beta|\langle\alpha|$ in the continuous-variable basis. Using

$$\text{Tr}\{\rho_-(\tau; \epsilon_1, \epsilon_2)\Pi\} = \sum_{n,m} \langle X_n|\rho_-(\tau)|X_m\rangle\langle X_m|D_1^\dagger(i\epsilon_1) \otimes D_2^\dagger(i\epsilon_2)\Pi D_1(i\epsilon_1) \otimes D_2(i\epsilon_2)|X_n\rangle, \tag{46}$$

\mathcal{B} is obtained by a straightforward calculation as

$$\mathcal{B} = \text{Ave}(\epsilon_1, \epsilon_2) + \text{Ave}(\epsilon_1, \epsilon'_2) + \text{Ave}(\epsilon'_1, \epsilon_2) - \text{Ave}(\epsilon'_1, \epsilon'_2), \tag{47}$$

$$\text{Ave}(\epsilon_1, \epsilon_2) = g(\epsilon_1, \epsilon_2)A + l(\epsilon_1, \epsilon_2)E + 2h(\epsilon_1, \epsilon_2)(C - D) + (j(\epsilon_1, \epsilon_2) + k(\epsilon_1, \epsilon_2))C, \tag{48}$$

$$g(\epsilon_1, \epsilon_2) = (2\mathbf{P}_e(\epsilon_1) - 1)(2\tilde{\mathbf{P}}_e(\epsilon_2) - 1), \tag{49}$$

$$h(\epsilon_1, \epsilon_2) = 8\mathbf{I}_e(\epsilon_1)\mathbf{I}_e(\epsilon_2), \tag{50}$$

$$j(\epsilon_1, \epsilon_2) = (2\mathbf{P}_e(\epsilon_1) - 1)(2\tilde{\mathbf{P}}_e(\epsilon_2) - 1), \tag{51}$$

$$k(\epsilon_1, \epsilon_2) = (2\mathbf{P}_e(\epsilon_1) - 1)(2\tilde{\mathbf{P}}_e(\epsilon_2) - 1), \tag{52}$$

$$l(\epsilon_1, \epsilon_2) = (2\mathbf{P}_e(\epsilon_1) - 1)(2\tilde{\mathbf{P}}_e(\epsilon_2) - 1), \tag{53}$$

where $\mathbf{P}_e(\epsilon) = \langle e'(\tau)|\Pi_e|e'(\tau)\rangle$, $\tilde{\mathbf{P}}_e(\epsilon) = \langle d'(\tau)|\Pi_e|d'(\tau)\rangle$, $\mathbf{I}_e(\epsilon) = \langle e'(\tau)|\Pi_e|d'(\tau)\rangle$, $\mathbf{P}_o(\epsilon) = \langle e'(\tau)|\Pi_o|e'(\tau)\rangle = 1 - \mathbf{P}_e(\epsilon)$, $\tilde{\mathbf{P}}_o(\epsilon) = \langle d'(\tau)|\Pi_o|d'(\tau)\rangle = 1 - \tilde{\mathbf{P}}_e(\epsilon)$, $\mathbf{I}_o(\epsilon) = \langle d'(\tau)|\Pi_o|e'(\tau)\rangle = -\mathbf{I}_e(\epsilon)$. These are modified versions of Eqs. (35) to (40) with $|e'(\tau)\rangle = D(i\epsilon)|e(\tau)\rangle$ and $|d'(\tau)\rangle = D(i\epsilon)|d(\tau)\rangle$. As α increases, it is expected that the result in 2×2 space under the $D(i\epsilon)$ operation approaches to the ideal case shown in Fig. 5.

Fig. 7 shows the largest Bell violation $|\mathcal{B}|_{max}$ for $\rho_-(\tau)$ against the normalised time. It is different from the former case of continuous variable entangled coherent state for $\tau \neq 0$, because the concerned identities are different from each other. The nonlocality of a given state can differ according to the Hilbert space concerned even though the same kind of measurement observable is used. For $\alpha \gg 1$, the rotation needed for the nonlocality test in the 2-qubit state is ideally realised, and the time variance of the nonlocality approaches to

the ideal case in Fig. 5 as was expected. For $\alpha \ll 1$, required rotation deviates from the ideal case.

V. REMARKS

We have studied the dynamic behavior of nonlocality for an entangled coherent state in a dissipative environment. The nonlocality test for an entangled coherent state can be realised with photon number measurement and displacement operations. Any entangled coherent state in the form of Eq. (2) can be transformed to a form (1) by local unitary transformations. The entangled coherent state is found to be nonlocal regardless of its amplitude. The higher the amplitude, the larger the nonlocality is. When the state interacts with its environment, the nonlocality is lost. The rapidity of the loss of nonlocality depends on the initial amplitude of the state. The larger the initial amplitude, *i.e.*, the larger the initial nonlocality, the more rapid the loss of nonlocality occurs. An entangled coherent state can be studied in 2×2 Hilbert space assuming a vacuum environment, where the nonlocality of the same state persists for longer in the dissipative environment.

ACKNOWLEDGMENTS

This work has been supported by the UK Engineering and Physical Sciences Research Council (GR/R33304). D.W. is grateful for financial support from the Department of Higher and Further Education Training and Employment (DHFETE) and the David Bates conference fund. H.J. acknowledges the Overseas Research Student award.

REFERENCES

- [1] A. Einstein, B. Podolsky and N. Rosen, *Phys. Rev.* **47**, 777 (1935).
- [2] S. Bell, *Physics* **1**, 195 (1964).
- [3] J. F. Clauser, M. A. Horne, A. Shimony and R. A. Holt, *Phys. Rev. Lett.* **23**, 880 (1969).
- [4] J. F. Clauser and M. A. Horne, *Phys. Rev. D* **10**, 526 (1974).
- [5] S. J. Freedman and J. F. Clauser, *Phys. Rev. Lett.* **28**, 938 (1972); A. Aspect, P. Grangier and G. Roser, *Phys. Rev. Lett.* **47**, 460 (1981).
- [6] G. Weihs, T. Jennewin, C. Simon, H. Weinfurter, and A. Zeilinger, *Phys. Rev. Lett.* **81**, 5039 (1998); A. Aspect, *Nature* **398**, 189 (1999).
- [7] A. Garg and N. D. Mermin, *Phys. Rev. D* **35**, 3831 (1987).
- [8] J. Larsson, *Phys. Rev. A* **57**, 3304 (1998).
- [9] A. Aspect, J. Dalibard and G. Roger, *Phys. Rev. Lett.* **49**, 1804-1807 (1982); P. R. Tapster, J. G. Rarity and P. C. M. Owens, *Phys. Rev. Lett.* **73**, 1923-1926 (1994); A. Aspect, *Nature* **398**, 189-190 (1999).
- [10] M. A. Rowe, D. Kielpinski, V. Meyer, C. A. Sackett, W. M. Itano, C. Monroe and D. J. Wineland, *Nature* **409**, 791 (2001) and references therein.
- [11] B. C. Sanders, *Phys. Rev. A* **45**, 6811 (1992); B. C. Sanders, K. S. Lee and M. S. Kim, *Phys. Rev. A* **52**, 735 (1995).
- [12] B. Yurke and D. Stoler, *Phys. Rev. Lett.* **57**, 13 (1986).
- [13] L. Davidovich, A. Maali, M. Brune, J. M. Raimond and S. Haroche, *Phys. Rev. Lett.* **71**, 2360 (1993).
- [14] S. J. van Enk and O. Hirota, *Phys. Rev. A* **64**, 022313 (2001).

- [15] O. Hirota and M. Sasaki, Phys. Rev. A **65**, 022319 (2002); O. Hirota, S. J. van Enk, K. Nakamura, M. Sohma and K. Kato, e-print quant-ph/0101096.
- [16] X. Wang, Phys. Rev. A **64**, 022303 (2001).
- [17] H. Jeong, M. S. Kim and J. Lee, Phys. Rev. A **64**, 052308 (2001).
- [18] K. E. Cahill and R. J. Glauber, Phys. Rev. **177**, 1857 (1969).
- [19] K. Banaszek and K. Wódkiewicz, Phys. Rev. A **58**, 4345 (1998).
- [20] K. Banaszek and K. Wódkiewicz, Phys. Rev. Lett. **99**, 2009 (1999).
- [21] H. Moya-Cessa and P. L. Knight, Phys. Rev. A **48**, 2479 (1993); B. -G. Englert, N. Sterpi and H. Walther, Pot. Commun. **100**, 526 (1993).
- [22] H. Jeong, J. Lee and M. S. Kim, Phys. Rev. A **61**, 052101 (2000).
- [23] B. S. Cirel'son, Lett. Math. Phys. **4**, 93 (1980).
- [24] N. Gisin, Phys. Lett. A **154**, 201 (1991).
- [25] W. H. Press, B. P. Flannery, S. A. Teukolsky and W. T. Vetterling, *Numerical Recipes* (Cambridge University Press, Cambridge, 1988).
- [26] W. J. Munro, G. J. Milburn and B. C. Sanders, Phys. Rev. A **62**, 052108 (2000); D. A. Rice, G. Jaegar and B. C. Sanders, Phys. Rev. A **62**, 012101 (2001).
- [27] S. L. Braunstein, A. Mann and M. Revzen, Phys. Rev. Lett. **68**, 3259 (1992).
- [28] R. Horodecki, P. Horodecki and M. Horodecki, Phys. Lett. A **200**, 340 (1995).
- [29] P. T. Cochrane, G. J. Milburn and W. J. Munro, Phys. Rev. A **59**, 2631 (1999); W. J. Munro, G. J. Milburn and B. C. Sanders, Phys. Rev. A **62**, 052108 (2000).
- [30] S. Popescu, Phys. Rev. Lett. **72**, 797 (1994); R. Horodecki, P. Horodecki and M. Horodecki, Phys. Lett. A **200**, 340 (1995).

[31] Z. Chen, J. Pan, G. Hou and Y. Zhang, Phys. Rev. Lett. , **88**, 040406 (2002).

[32] W. J. Munro, K. Nemoto and A. G. White, J. Mod. Opt., **48**, 1239 (2001).

FIGURES

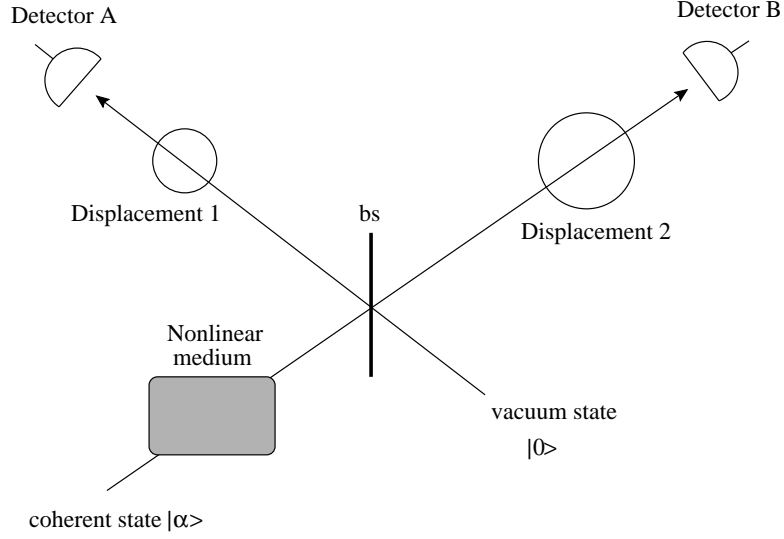


FIG. 1. Nonlocality test for an entangled coherent state. A coherent state, nonlinear medium, and 50-50 beam splitter are used to generate an entangled coherent state.

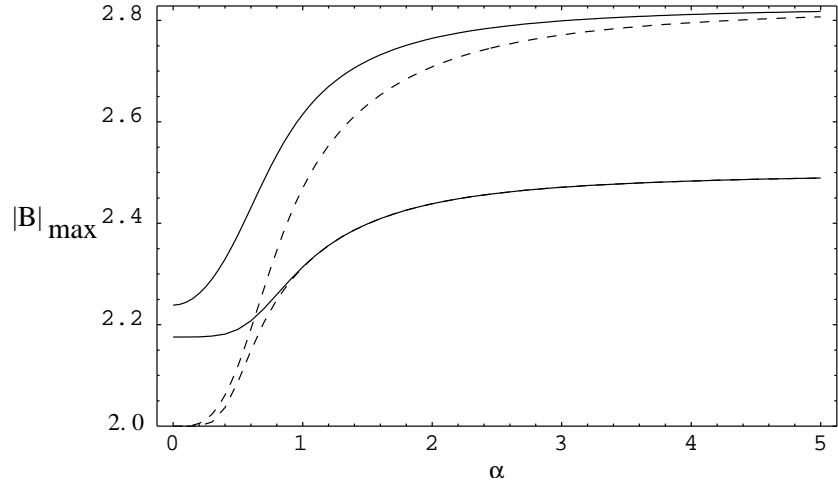


FIG. 2. Bell measure against amplitude α (> 0), of $|C_{-}\rangle$ (solid lines) and $|C_{+}\rangle$ (dashed lines) entangled coherent states. The higher valued solid and dashed lines are for the generalised Bell measures while the lower valued solid and dashed lines are for the case taking $\alpha = \beta = 0$.

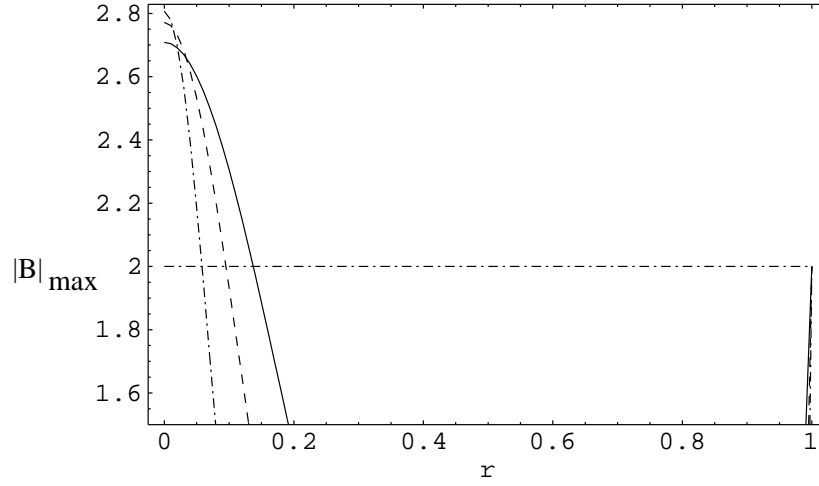


FIG. 3. Nonlocality as a function of the dimensionless normalised time r for the $|C_{-}\rangle$ state in the vacuum. $\alpha = 2$ (solid line), $\alpha = 3$ (dashed line) and $\alpha = 5$ (dot-dashed line).

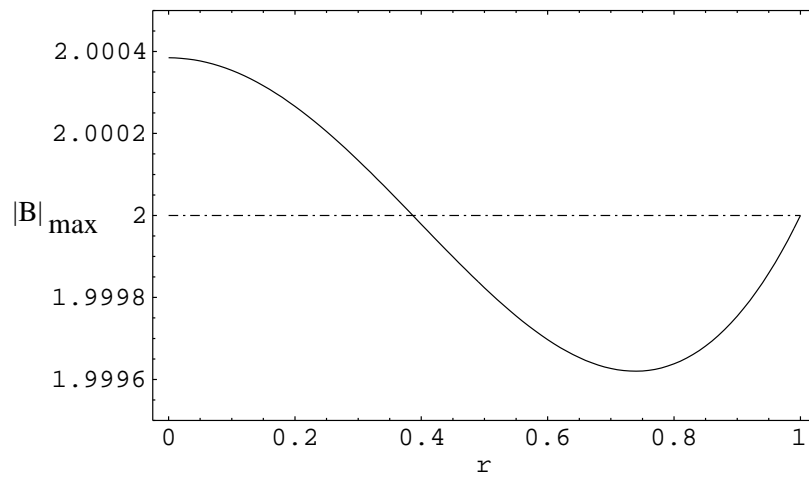


FIG. 4. The $|C_{+}\rangle$ state for the coherent amplitude $\alpha = 0.1$, coupled to the vacuum environment, produces a prolonged nonlocal state.

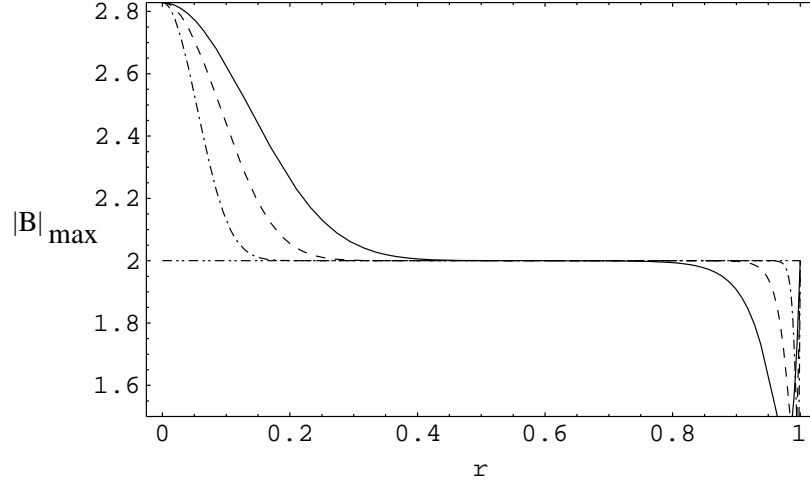


FIG. 5. Bell measure for an entangled coherent state against normalised time r in 2×2 Hilbert space under perfect rotations. Nonlocality persists longer in 2×2 space than in continuous Hilbert space. $\alpha = 2$ (solid line), $\alpha = 3$ (dashed line) and $\alpha = 5$ (dot-dashed line).

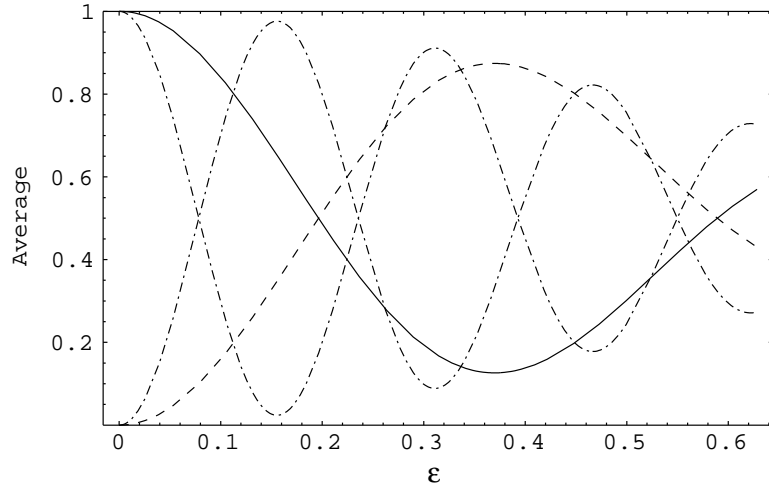


FIG. 6. Oscillations in even and odd states by the displacement operator $D(i\epsilon)$. For $\alpha \gg 1$, the displacement operator acts as a sinusoidal rotation. For $\alpha = 2$, $\langle e' | \Pi_e | e' \rangle$ (solid line) and $\langle d' | \Pi_e | d' \rangle$ (dashed line). For $\alpha = 5$, $\langle e' | \Pi_e | e' \rangle$ (dot-dashed line) and $\langle d' | \Pi_e | d' \rangle$ (dotted line).

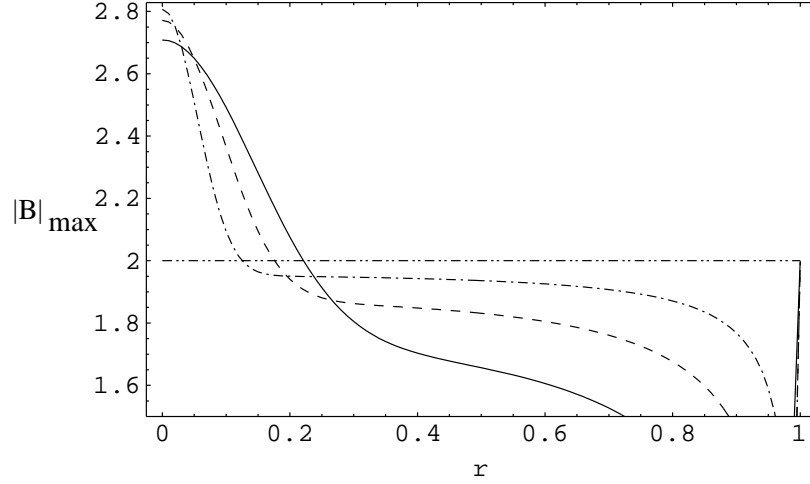


FIG. 7. Bell measure against normalised time for a mixed entangled coherent state in 2×2 Hilbert space. For $\alpha \gg 1$, rotation needed for the nonlocality test in the 2-qubit state is ideally realised as shown in Fig. 6, and the Bell function approaches the ideal case shown in Fig. 5. $\alpha = 2$ (solid line), $\alpha = 3$ (dashed line) and $\alpha = 5$ (dot-dashed line).